AD-711-316

This document has been approved for public release and sale; its distribution is unlimited.

NUCLEAR EMULSION RECORDINGS OF THE ASTRONAUTS' RADIATION EXPOSURE ON THE FIRST LUNAR LANDING MISSION APOLLO XI*

Hermann J. Schaefer and Jeremiah J. Sullivan

Bureau of Medicine and Surgery
MF 12.524.010-5001B

Approved by

Ashton Graybiel, M.D.
Assistant for Scientific Programs

Released by

Captain N. W. Allebach, MC USN
Officer in Charge

29 June 1970

*This work was conducted under contract with the Manned Spacecraft Center, National Aeronautics and Space Administration, Houston, Texas.

NAVAL AEROSPACE MEDICAL RESEARCH LABORATORY
NAVAL AEROSPACE MEDICAL INSTITUTE
NAVAL AEROSPACE MEDICAL CENTER
PENSACOLA, FLORIDA 32512

Best Available Copy

SUMMARY PAGE

THE PROBLEM

As on all earlier Apollo missions, the astronauts on the first lunar landing mission Apollo XI carried passive dosimeter packs on chest, thigh, and ankle, containing nuclear and ordinary film badge emulsions, thermoluminescent powder, Lexan foils, and neutron activation foils. Of these different radiation sensors, the nuclear emulsions are of special importance since they allow determination of particle types and energy spectra of the various constituents of the radiation environment in space. This report is limited to a presentation of the findings with nuclear emulsions.

FINDINGS

For reasons of time economy, one pack (Neil Armstrong, Commander, Ankle) was selected for a complete track and grain count analysis of the G.5 and K.2 emulsions supplemented by an endom count in the K.2. A proton dose of 151 millirad or 220 millirem was found. For all other packs, merely endom counts were carried out in the K.2 emulsions; these were found to vary between 35 and 42 endom/mm^2, normalized to 200-micron thickness of unprocessed emulsion. By applying Yagoda's method, the star frequency in the gelatin matrix of the K.2 emulsions was established from the integral prong spectrum and furnished a dose contribution from disintegration stars in tissue of 15 millirad or 94 millirem. The dose from fast neutrons was estimated at 1.2 millirad or 12 millirem from the count of recoil protons. Only a coarse estimate of the dose contribution from electrons and gamma rays was possible by comparing the blob count of terminating electrons in the flown emulsions to the one in the sea-level controls. The dose was estimated at about 30 millirad which is identical to the millirem dose. The scan for heavy nuclei was limited to tracks with Z numbers of 22 or greater. The flux of the medium and low Z part of the heavy spectrum was assessed theoretically from the measured flux in the heaviest class according to Z abundances reported in the literature. A total absorbed dose of 5.3 millirad from heavy nuclei was obtained. Applying conventional QF values to the contributions of the various Z groups furnishes a dose equivalent of 46 millirem although this cannot be considered an adequate expression of the microbeam effectiveness of high ZE particles in tissue. The indicated contributions furnish a grand total mission dose of 201 millirad or 402 millirem.

INTRODUCTION

The first lunar landing mission Apollo XI was launched on 16 July 1969 and splashed down on 24 July after a total mission time of 195.3 hours. As on all earlier missions, the astronauts on Apollo XI were equipped with a variety of radiation dosimeters and survey meters so that they would be prepared for all contingencies and could carry out, at any time, in-flight readings of instantaneous skin and depth dose rates as well as accumulated doses (1). In addition to these active dosimeters, the astronauts carried, in pouches in their constant-wear garments on chest, thigh, and ankle, passive dosimeters for post-flight analysis of the total mission exposure. These radiation packs contained nuclear and ordinary film badge emulsions, thermoluminescent material, Lexan foils, and neutron activation foils. Of these sensors, the nuclear emulsions are of unique importance since they furnish a permanent record of all nuclear particles which have entered or left the astronaut's body at the location of the pack. The following report is limited to the findings from the nuclear emulsions and presents the results of the microscopic track counting which had been accumulated when the scanning effort had to be switched to the emulsions of Apollo XII.

Aside from the nonphotographic materials mentioned above, the packs contained varying combinations of Ilford G.5 emulsions of 25 and 50 and 100 micron thickness and K.2 emulsions of 100 micron, ordinary Eastman Kodak double-component film badge emulsions, and Eastman Kodak personal neutron monitoring emulsions. As with the nuclear emulsions of earlier manned missions, three different types of data were established in separate scanning runs. These were track and grain counts in G.5 and K.2 emulsions, proton ender and neutron recoil counts in K.2 emulsions, and heavy nuclei counts in G.5 emulsions. A combined evaluation of these data ensured sustained resolution of energy over a very wide range essentially down to zero Mev (ender) and allowed determination of the total mission dose both in terms of absorbed dose (millirad) and dose equivalent (millirem). The details of the three methods have been described in a number of earlier publications (2-6).

On deep-space missions, the galactic contribution accounts for a substantially larger part of the total mission dose equivalent than it does on a standard near-Earth orbital mission of low inclination. This basic difference became strikingly apparent when the emulsion data of the near-Earth orbital mission Apollo VII were compared to those of the first lunar mission Apollo VIII as described in a preceding report (7). As a consequence of the greater importance of galactic radiation on a deep-space mission, the dose contribution from so-called disintegration stars released mainly by high-energy galactic protons and neutrons in the body tissues themselves likewise assumes sizeable proportions and can no longer be disregarded. Data on this component are presented in the present report for the first time. Although the star counts are collected together with the ender and recoil counts, it might be more appropriate to consider the star data as a separate fourth set in addition to the three conventional ones mentioned above.

DOSE CONTRIBUTION FROM TRAPPED PROTONS

A major portion of the astronauts' radiation exposure on a lunar mission is due to trapped protons encountered in two passes through the radiation belt. The flux density of protons is highest in a comparatively narrow region of the so-called inner belt about the geomagnetic equator. It drops steeply toward higher latitudes. Therefore, the radiation levels encountered on translunar and trans-Earth injection sensitively depend on the particular geomagnetic trajectories of a mission. Since the planes of the geomagnetic equator and the Moon's orbit about the Earth show a continuously varying angle of inclination, the trajectories in question vary from mission to mission depending on the particular angle of inclination at the time of passage. The indicated conditions were exceptionally favorable on both passages of the Apollo XI mission, yet rather unfavorable on trans-Earth injection on Apollo XII.

Figure 1* shows the geomagnetic trajectories through the inner radiation belt for the two missions Apollo XI and XII. The coordinate system is so-called B, L space in which the geomagnetic equator appears as a hyperbola and all longitudinal asymmetries, which the magnetic field of the Earth shows in geographic coordinates, disappear. It is seen from Figure 1 that the return trajectory of Apollo XII passed very closely to the center of the inner belt with flux densities in excess of 4,000 protons/cm^2 sec, whereas on Apollo XI the outgoing trajectory came closest to the center yet still brushed only briefly the 500 proton/cm^2 sec isoflux line. In terms of Earth-Moon distance, the high radiation area of the inner belt is still in very close vicinity of the Earth. Therefore, the vehicle travels at practically full escape or reentry velocity as it passes through. This circumstance in connection with the heavy inherent shielding of the Apollo vehicle keeps the radiation exposure from trapped protons on a surprisingly low level.

As mentioned before, the details of the evaluation of the proton dose from track and grain counts in G.5 and enders counts in K.2 have been described in reports on earlier missions. [The reader is especially referred to the report on the Apollo VII mission (6).] In the present report on Apollo XI, we limit ourselves to a presentation of the final results. For reasons of time economy, only one pack (S/N 135, Commander, Ankle) was subjected to a full track and grain count of the G.5 and K.2 emulsion sheets. Table I presents the data already expressed in LET classes. A total of 1957 tracks in the G.5 and 2034 tracks in the K.2 emulsion were grain counted and their respective lengths determined. An area of 7.2 mm^2 of the K.2 emulsion in the center of the film sheet was scanned for proton enders.

The differential flux in high LET classes shows major local variations reflecting variations of the local shield distribution. At the same time, grain counting in these LET

- - - - - - - - - - -

*In order not to break the continuity of the text, all tables and illustrations appear at the end.

classes is less accurate because of grain crowding which makes itself felt even in the K.2 for the three highest LET classes. Therefore, the LET classes beginning with 9.80 kev/micron tissue were evaluated by establishing the grand total track length for these classes and redistributing the total into individual classes according to a curve of smooth fit with the enders count as anchor point at the upper end of the LET scale. This is the reason why in Table I only the total flux for the seven highest LET classes is shown since only this flux is based directly on the raw scores.

Determining the flux densities in the high LET classes as accurately as possible is of special importance because these classes contribute most heavily to the total dose. Moreover, they furnish the dose fraction to which QF values of 3.0 and larger would have to be assigned if absorbed doses are to be converted to dose equivalents. The latter circumstance further enhances the weight of this particular fraction of the total flux. How heavy this weight already is in terms of absorbed dose is well demonstrated in Figure 2 which shows the data of Table I in two histograms, the lower one pertaining to flux densities and the upper one to the corresponding absorbed doses in millirad. Contrary to the presentation in Table I, a QF limit of 2.0 was selected in Figure 2; thus the eight highest LET classes are lumped together into one bar. It should be obvious that simply applying a mean QF to the bulk dose of the right-hand bar would introduce a large margin of uncertainty into the assessment of the dose equivalent. The QF values listed in Column 5 of Table I correspond to the mean LET values of the class limits in Columns 1 and 2 and have been established according to the recommendations in Publication 9 of the International Commission of Radiological Protection (ICRP) (8). Below Columns 4 and 6 in Table I the grand totals, 150.7 millirad and 220.0 millirem, respectively, are listed. Although it has been mentioned in all earlier reports, it should be expressly mentioned again that these doses, which we loosely call proton doses, actually contain a small undetermined fraction from alpha particles and a still smaller fraction from low-Z heavy nuclei.

As mentioned before, the just-reported complete analysis of the proton dose pertains to the G.5 and K.2 emulsions of only one pack. For the eight other packs carried by the astronauts and for the extra pack carried in the film bag, only enders and star counts were done. The enders counts varied from a lowest value of 35 enders/mm^2 in 200-micron K.2 emulsion to a highest of 42/mm^2. Since the enders count is representative of the flux fraction of lowest penetration, it shows substantially larger variations than the total flux. Therefore, the total proton doses at the eight locations must have varied less than the enders counts. The enders count in the K.2 emulsion of Pack S/N 135, which was subjected to the complete track and grain count analysis just presented, was 40.0 enders/mm^2 normalized to a thickness of 200 micron of unprocessed emulsion.

DOSE CONTRIBUTION FROM TISSUE DISINTEGRATION STARS

As mentioned before, the dose from trapped protons on Apollo XI was exceptionally low due to near-optimum trajectory parameters in both passages through the inner radiation belt. This means that all other contributions to the mission dose are enhanced

Figure 3 shows the data of Table II in a semilog plot. The characteristic discontinuity in the slope at prong number 7 is clearly seen. The broken line indicates the straight-line extrapolation of the integral prong spectrum as it would hold without the gelatin furnishing additional stars below prong number 7. The difference of the extrapolated and the actually observed integral spectrum, then, must represent the star contribution from the gelatin matrix of the emulsion. This contribution is shown separately in Figure 3.

A special problem in the evaluation of the energy deposited by stars is posed by the 2-prong stars. Many 2-prong stars are difficult to identify in the scan and will be misinterpreted as ordinary proton enders showing nuclear scattering. In other words, their energy contribution is already accounted for properly in the enders dose. Other 2-prong stars will appear as "through shots," hence will be accounted for in the general proton dose. It is seen, then, that inclusion of the 2-prong stars as obtained by differential extrapolation of the prong spectrum in the dose contribution from tissue stars would lead to double accounting for a large fraction of them. Accepting a slight underrating of the total energy dissipation as the lesser error, we have disregarded, in assessing the dose contribution from tissue stars, the 2-prong stars altogether.

An easy calculation furnishes the value of 3.95 as the mean prong number per star for all gelatin stars with three or more prongs from the data in Table II. This value is about 6 per cent larger than the value of 3.7 which Yagoda reports for his emulsions flown with balloons. In view of the different galactic spectra at balloon altitudes and in deep space, the agreement must be considered very satisfactory. Applying the values quoted earlier for the mean "energy" and "damage" per prong to the prong population of gelatin stars in Table II and remembering that the gelatin matrix occupies very nearly half the total volume of unprocessed emulsion, we arrive at doses of 15 millirad or 94 millirem from disintegration stars in tissue. It is seen that the star phenomenon on a deep-space mission indeed contributes significantly to the total mission dose.

Besides charged particles, neutrons are generated in disintegration stars. Since neutrons themselves do not ionize, their paths do not appear as visible prongs in nuclear emulsion. Quite generally, the mechanism of energy dissipation for neutrons is completely different from the one for charged particles. Imparting their kinetic energy in elastic collisions mainly to hydrogen nuclei in the absorbing medium, fast neutrons emitted from stars gradually slow down until they are finally captured in nuclear reactions. As a consequence, neutrons diffuse out to much greater distances from the center of the disintegration where they have originated. Therefore, the energy of neutrons from a star cannot be considered as dissipated locally, and it would be erroneous to add the energy to that from the short-ranged protons and alpha particles in assessing the local star dose. At any location in an emulsion layer, the local neutron flux density reflects an equilibrium state, with a substantial fraction of the flux originating in star events millimeters or even centimeters away in the materials surrounding the emulsion.

The source spectra of neutrons originating in nuclear interactions of galactic primaries as well as the degradation of these spectra in matter have been extensively

investigated, and it is well established that the bulk of the local equilibrium flux centers heavily on a narrow energy interval around 1 Mev. In tissue in particular, fast neutrons in the energy region about 1 Mev dissipate their energy mainly through recoil protons which they produce in elastic collisions with hydrogen atoms in tissue. "Tissue equivalent" recoil protons also originate in the gelatin matrix of emulsion and appear under the microscope as short tracks. Since the counting of these tracks, although somewhat time consuming, is basically a simple technique of measuring flux density and absorbed dose from fast neutrons, considerable efforts have been devoted by many investigators toward establishing an empirical constant linking the track count to the absorbed dose (14). For the 30-micron NTA emulsion of Eastman Kodak Neutron Monitoring film, this constant is 18 recoil tracks per cm^2 emulsion area for an exposure of 0.1 millirad from fast neutrons.

In neutron measurements with nuclear emulsions in space, complications arise due to the fact that numerous tracks from trapped protons in the radiation belt are superimposed on the neutron recoil proton tracks. There is no immediate criterion available by which the two kinds of tracks could be distinguished. Merely those proton tracks that originate and end in the emulsion, so-called suspended tracks, can be safely excluded as being from trapped particles. Protons ending in the emulsion yet entering from the outside cannot be classified with certainty as to their origin. However, since the neutron energy spectrum centers heavily on 1 Mev, recoil protons with initial energies exceeding a few Mev are quite rare. Therefore, enders entering the emulsion from the outside with higher energies, i.e., enders of a sufficient length, can safely be excluded as neutron recoils.

In 7.2 mm^2 of scanned emulsion area of the 100-micron K.2 in Pack S/N 135, 50 suspended tracks were counted. Applying the just-quoted empirical constant to this count, we arrive at an absorbed dose of 1.2 millirad corresponding to a dose equivalent of 12 millirem from fast neutrons. This value might be slightly low because the efficiency in recognizing short tracks begins to drop below 100 per cent from about 0.5 Mev down to lower energies because of the background of terminating electrons and other small grain deposits in the emulsions. We therefore would prefer to call the quoted values estimates rather than precise figures. However, we feel that they underestimate the dose contribution from fast neutrons by much less than a factor of 2 and disprove the assumption sometimes made that neutrons are a major factor in the astronauts' radiation exposure.

DOSE CONTRIBUTION FROM HEAVY NUCLEI

The greater importance of galactic radiation for the astronauts' radiation exposure on a deep-space mission was shown in the preceding section where the dose contribution from disintegration stars in tissue was analyzed. It becomes all the more obvious when we investigate the flux densities of heavy particles, or "high ZE particles" as they now are called. The different magnitude of the heavy flux in deep space became strikingly apparent when the heavy nuclei counts of the standard near-Earth orbital mission Apollo VII were compared with those of the first lunar mission Apollo VIII. An earlier report (7) deals exclusively with these findings. It gives a detailed description

of the scanning method and discusses the flux data and the problem of their dosimetric interpretation. Since we have applied, in scanning the Apollo XI emulsions for high ZE particles, the same method and used the same reference standards for Z determination, the reader is referred to this earlier account with regard to all details of the evaluation procedure.

Figures 4 through 10 show micrographs of typical high ZE particle tracks in the emulsions flown on Apollo XI. They are selected in an attempt to convey an idea of the great variety of particles which hide under the common name high ZE particles. Figure 4 shows a low-power field with three heavy particles in close vicinity. Their Z numbers are estimated as 8, 10, and 18. The reader who would want to visualize these three nuclei traversing cellular tissue instead of nuclear emulsion is reminded that the stopping power of emulsion is roughly twice that of tissue. In other words, all linear distances measured in the emulsion micrograph would be twice as long in tissue. Figure 5 shows another field with three heavy particles closely together, taken at higher power than Figure 4. The Z numbers are estimated as 10, 12, and 16. Figure 6 shows a single heavy track with an estimated Z number of 22. Figure 7 shows the heaviest track recorded on mission Apollo XI; estimated Z number is 28 to 30. Figure 8 shows a track which penetrates the emulsion at a steeper angle. Accordingly, the track is in sharp focus only for about one-fourth to one-fifth of its full length. The projective shortening of steep angle tracks makes them appear heavier than they would at a flat angle. Taking this distortion into consideration, we estimate the Z number at 22 to 26.

Finally, Figure 9 and 10 show an ender or "thindown," i.e., the track of a nucleus which comes to rest in the emulsion. The coherent terminal section of the track has been broken into four parts. The track begins at the upper right-hand corner in Figure 10, with lower ends connecting to adjacent upper corner to the left. Whereas the tracks in Figures 4 to 8 are all from G.5 emulsions, the ender in Figures 9 and 10 was found in K.2 emulsion. The much lower sensitivity of the K.2 is easily recognized by comparing the general background in the micrographs. Because of this lower sensitivity, the width of the solid silver core and the delta aura appear also much smaller than they would in G.5. The Z of the ender is estimated at 22.

Table III shows the result of the heavy counts. Actual scans were carried out only for the highest Z class covering the interval from Z = 22 to 30. The fluxes in the three lower classes were established theoretically using values for the relative Z abundances reported in the literature. Dose equivalents were computed by applying QF values according to the recommendations of the ICRP. In establishing the dose contributions it was assumed that all particles are of high energy travelling at near-relativistic speed. In other words, minimum LET values used were obtained by multiplying the minimum LET of protons by Z^2. This method underrates the true exposure because a certain fraction of the heavy flux is made up of particles of lower energies for which the LET would be larger than Z^2 times the proton minimum.

Low-energy particles pose a new problem on deep-space missions which did not exist for near-Earth orbital missions of low inclination. Outside the magnetosphere in

deep space, the galactic spectrum is different from the truncated spectrum in near-space at low geomagnetic latitudes. The influence of the geomagnetic field is explained in Figure 11. It shows the differential energy spectra for the $Z \geq 20$ group at solar minimum and maximum. Available data in the literature on the effects of solar modulation on the low-energy section of the galactic spectrum show some discrepancies. The spectra in Figure 11 represent a compromise between the data of Webber (15) and those of Balasubrahmanyan and co-authors (16). On a near-Earth orbital mission of 31.5° geographic inclination, the geomagnetic inclination oscillates between 20° and 43° because the rotational and geomagnetic axes are inclined 11.5° toward each other. As a consequence, the geomagnetic cut-off energy also oscillates, limiting the allowed spectrum reaching the vehicle to the shaded portions of the figure.

Since the Apollo XI mission was flown very nearly at solar maximum, we concentrate now on that curve in Figure 11, redrawing it at a larger scale in Figure 12. Outside the magnetosphere, there is no cut-off effect and the vehicle encounters the full spectrum. Low-energy particles now have free access. As a consequence, some of the particles will reach the end of their ionization ranges within the emulsions or the body tissues themselves. Since the attenuation mechanism of heavy nuclei in matter is well understood, the fraction of the incident flux which can escape nuclear collision and reach the "natural" end of its range can be assessed theoretically when the incident energy spectrum is known. The shaded area in Figure 12 represents this flux.

Two features of the spectrum of the enders flux are of special importance. Firstly, the spectrum is essentially outside and below the lowest cut-off energy for a standard near-Earth orbit. That means this type of heavy particle with an extremely high LET value in the Bragg peak is essentially excluded from near-Earth orbital missions. This conclusion is confirmed by our observations. We see heavy nuclei enders or thinlowns in the emulsions only on lunar missions. Secondly, the enders flux constitutes only a small fraction of the total heavy flux, as can be seen by comparing the respective areas of the enders flux and the total flux in Figure 12. This conclusion is also confirmed by our observations. Among the total population of heavy tracks in an emulsion from a lunar mission, we see only very few enders. In fact, the percentage of enders is even much smaller than could be expected from the respective areas in Figure 12. This finding indicates that the inherent heavy shielding of the Apollo vehicle affords substantial protection from this particularly undesirable section of the heavy spectrum.

Radiobiologically, the significance of the high ZE particles centers on the fractional flux with very high LET values. From what has just been discussed, this fractional flux is bound to depend sensitively on the local shield distribution in a similar fashion, as this is the case for the enders in the flux of trapped protons. However, as long as no clues are available as to the critical LET value beyond which expressing heavy-nuclei exposure in millirad or millirem becomes meaningless, the influence of shielding cannot be analyzed. So far, all attempts to propose new dosimetric units for microbeam exposure have been inadequate. One could speculate that one parameter in such a new dosimetric concept will be the frequency of discrete events per unit tissue volume. Since the nuclear emulsions flown on deep-space missions are permanent records

of all high ZE particles, they will lend themselves easily to a reassessment of the astronauts' radiation exposure at any time in the future when a dosimetric unit will be defined.

As we approach the final task of adding up the grand total mission dose for Apollo XI, a dose contribution has to be mentioned for which merely an estimate can be made from nuclear emulsions. We mean the dose from electrons and associated gamma rays. Although we know very well the densitometric response of the various emulsion types, nuclear as well as ordinary, in the radiation packs to Cobalt 60, radium gamma, and x-rays, the superimposed nuclear tracks in the emulsions flown in space prevent any densitometric evaluation of the dose contribution in question. Such evaluation would also encounter principal objections because of the greatly different energy spectra of electrons and gamma rays in space. The only clue available is that the number of tortuous heavy blobs which terminating electrons produce in G.5 and, with a thinner pattern, in K.2 emulsion is, for Apollo XI, in the flown emulsion about twice as large as in the sea-level controls. This would indicate that the exposure from electrons must have been small. We estimate that exposure at 30 millirad and millirem.

As all sources of exposure have now been discussed, we present in Table IV the summary of all contributions and the grand total mission dose itself without further comments.

Best Available Copy

REFERENCES

1. Berry, C. A., Summary of medical experience in the Apollo 7 through 11 manned spaceflights. Aerospace Med., 41:500-519, 1970.

2. Schaefer, H. J., Radiation monitoring on Project Mercury: Results and implications. Aerospace Med., 35:829-833, 1964.

3. Schaefer, H. J., and Sullivan, J. J., Radiation monitoring with nuclear emulsions on Mission Gemini IV and V. Aerospace Med., 38:1-5, 1967.

4. Schaefer, H. J., Messungen der Protonendosis der Gemini-Astronauten mit Kernemulsionen. Biophysik, 4:63-76, 1967.

5. Schaefer, H. J., and Sullivan, J. J., Radiation monitoring with nuclear emulsions on Project Gemini. II. Results on the 14-day mission Gemini VII. NAMI-990. NASA Manned Spacecraft Center. Pensacola, Fla.: Naval Aerospace Medical Institute, 1967.

6. Schaefer, H. J., and Sullivan, J. J., Nuclear emulsion measurements of the astronauts' radiation exposure on Apollo VII. NAMI-1060. NASA Manned Spacecraft Center. Pensacola, Fla.: Naval Aerospace Medical Institute, 1969.

7. Schaefer, H. J., and Sullivan, J. J., Nuclear emulsion recordings of heavy primaries on Apollo VII and VIII. NAMI-1091. NASA Manned Spacecraft Center. Pensacola, Fla.: Naval Aerospace Medical Institute, 1969.

8. Recommendations of the International Commission on Radiological Protection, Radiation Protection. ICRP Publication 9. New York: Pergamon Press, 1966.

9. Birnbaum, M., Shapiro, M. M., Stiller, B., and O'Dell, F. W., Shape of cosmic-ray star-size distributions in nuclear emulsions. Phys. Rev., 86:86-89, 1952.

10. Yagoda, H., Behar, A., Davis, R. L., Kramer, K. L., Filz, R., Hewitt, J., and Haymaker, W., Brain study of mice exposed to cosmic rays in the stratosphere and report of nuclear emulsion monitoring in four balloon flights from Bemidji, Minnesota July-August, 1960. Military Med., 128:655-672, 1963.

11. Harding, J. B., The origin of cosmic ray stars. Philosophical Mag., 42:63-73, 1951.

12. Powell, C. F., Fowler, P. H., and Perkins, D. H., The Study of Elementary Particles by the Photographic Method. New York: Pergamon Press, 1959.

13. Davison, P. J. N., Radiation dose rates at supersonic transport altitudes. M.O.A. Grand PD/34/017. Farnborough, Hampshire, England: Royal Aircraft Establishment, 1967.

14. Dudley, R. A., Dosimetry with photographic emulsions. In: Attix, F. H., and Roesch, W. C. (Eds.), Radiation Dosimetry. Vol. II. Instrumentation. New York: Academic Press, 1966. Pp 325-387.

15. Webber, W. R., Time variations of low rigidity cosmic rays during the recent sunspot cycle. In: Wilson, J. G., and Wouthuysen, S. A. (Eds.), Progress in Elementary Particle and Cosmic Ray Physics. Vol. VI. New York: John Wiley & Sons, 1962. Pp 75-243.

16. Balasubrahmanyan, V. K., Boldt, E., and Palmeira, R. A. R., Solar modulation of galactic cosmic rays. J. Geophys. Res., 72:27-36, 1967.

Table I

Evaluation of Absorbed Dose and Dose Equivalent From Track, Grain, and Ends Counts in G.5 and K.2 Emulsions of Rack S/N 135

LET-Interval kev/micron T	kev/micron T	Equivalent Unidirect. Flux, Protons/cm²	Absorbed Dose, millirads	QF	Dose Equivalent, millirems
0.20	0.27	567,300	22.7	1.0	22.7
0.27	0.35	215,750	11.8	1.0	11.8
0.35	0.43	165,100	11.4	1.0	11.4
0.43	0.52	91,950	7.75	1.0	7.75
0.52	0.615	65,700	6.63	1.0	6.63
0.615	0.715	65,700	7.77	1.0	7.77
0.715	0.84	41,250	5.71	1.0	5.71
0.84	1.15	81,280	14.4	1.0	14.4
1.15	1.67	40,100	10.0	1.0	10.0
1.67	2.52	20,580	7.67	1.0	7.67
2.52	4.00	14,760	8.49	1.0	8.49
4.00	7.70	14,040	13.0	1.6	20.8
7.70	9.80	7,480	11.6	2.35	27.4
9.80	13.2			3.0	
13.2	19.3			4.0	
19.3	26.3			5.3	
		4,290	11.8		57.5
26.3	37.9			7.3	
37.9	47.5			9.3	
47.5	60.6			11.0	
60.6	85.0			12.6	
		Total	150.7	Total	220.0

Table II

Prong Spectrum of Disintegration Stars in Ilford K.2 Emulsions of Apollo XI

Number of Prongs	Total Emulsion: Number of Stars Recorded	Total Emulsion: Integral Number of Stars	Gelatin Only: Number of Stars in Class	Gelatin Only: Integral Number of Stars
2	390	1395	200	500
3	309	1005	130	300
4	195	696	85	170
5	147	501	55	85
6	93	354	30	30
7	53	261	0	0
8	43	208	0	0
9	34	165	—	—
10	36	131	—	—
11-15	70	95	—	—
16-24	25	25	—	—

Emulsion area: 257.9 mm^2

Emulsion volume (unprocessed): 0.0258 cc

Table III

Heavy Nuclei Exposure on Apollo XI

Z-Class	Flux, Nuclei/cm^2	Absorbed Dose, millirad	Dose Equivalent, millirem
6-9	465	0.81	2.0
10-12	515	2.2	11.0
13-21	84	0.76	7.6
22-30	76	1.56	25.0
	Mission dose	5.33	45.6

Mission duration: 8.14 days

Table IV

Mission Dose and Its Components on Apollo XI

Component	Absorbed Dose, millirad	Dose Equivalent, millirem
Protons	150	220
Stars	15	94
Fast neutrons	~ 1	~ 12
Heavy nuclei	5	46
Electrons and gamma rays	~ 30	~ 30
Total	201	402

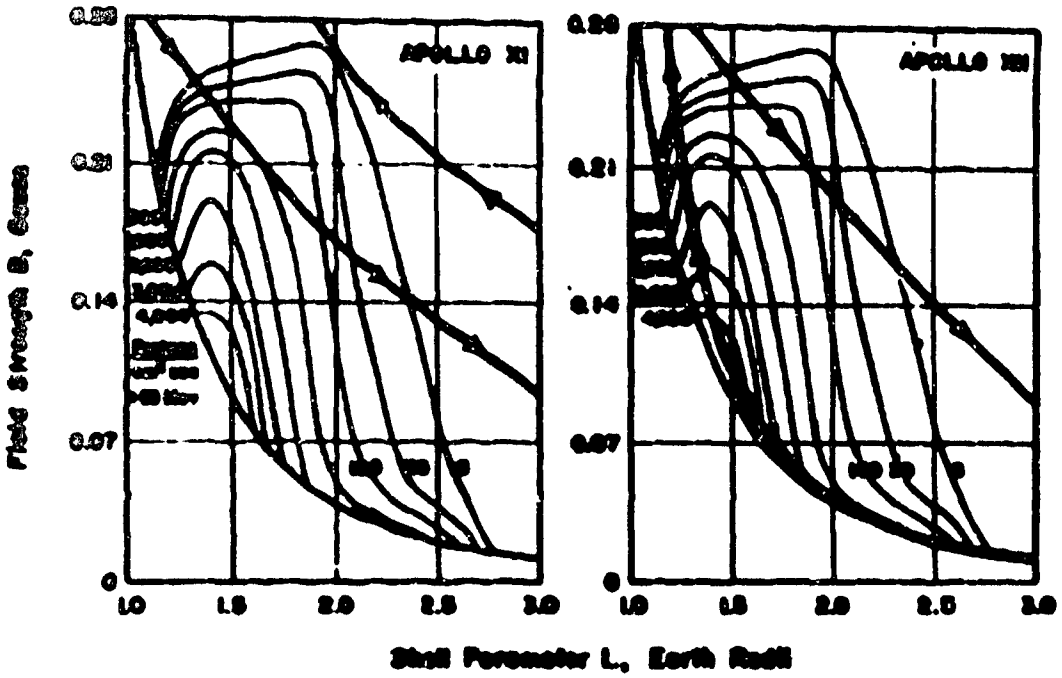

Figure 1

B, L Space Trajectories in Radiation Belt on Translunar and Trans-Earth Injection of Missions Apollo XI and XII

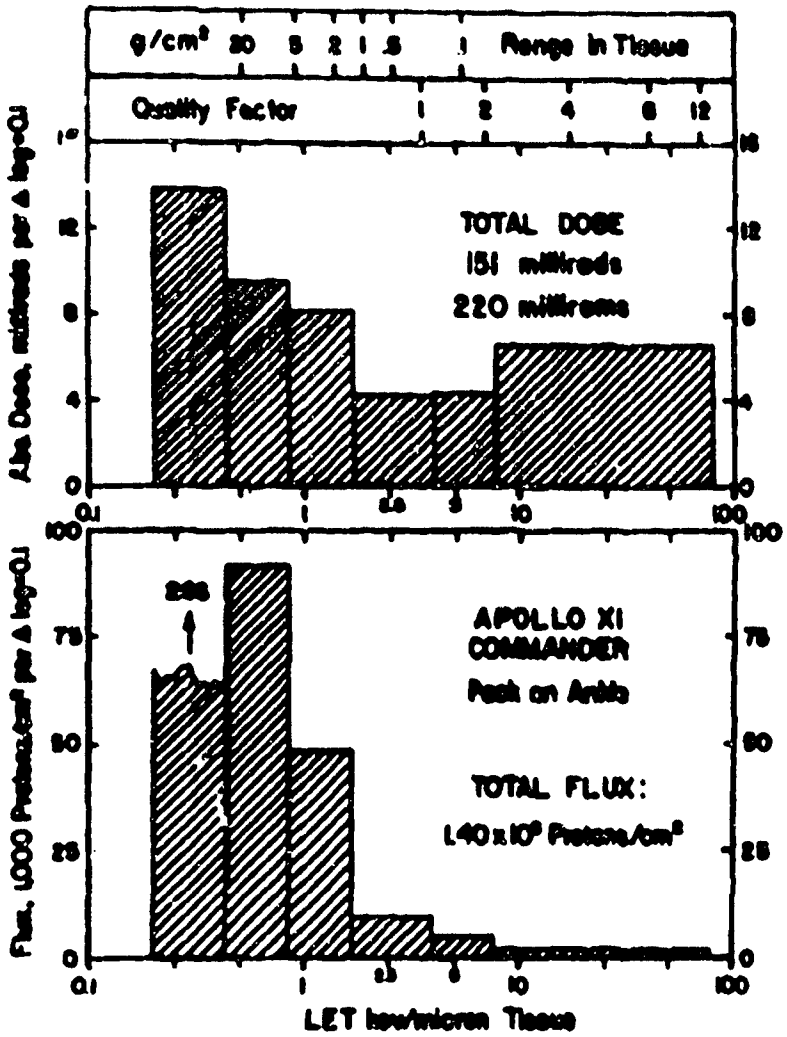

Figure 2

LET Distributions of Protun Flux and Absorbed Dose Established From Track, Gamin, and Enders Counts in G.5 and K.2 Emulsions of Pack S/N 135

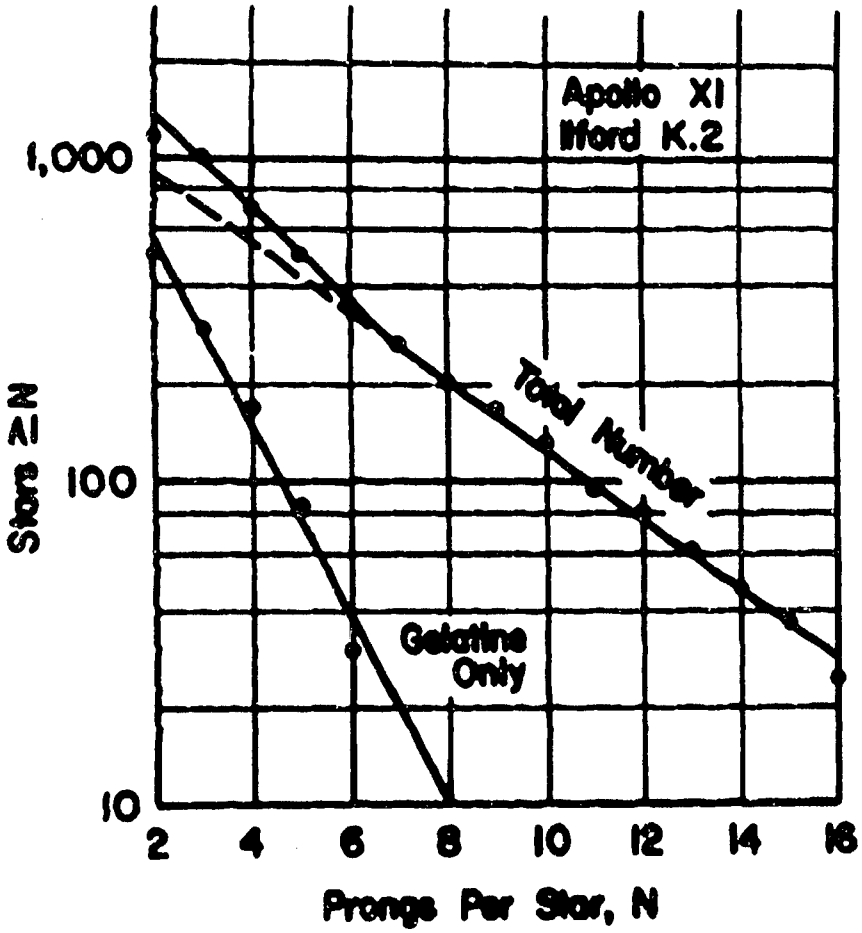

Figure 3

Integral Prong Spectrum for Star Population in K.2 Emulsions and Resulting Spectrum for Gelatin Stars

Figure 4

Micrograph From a G.5 Emulsion Showing Three Heavy Tracks In Close Vicinity

Field Size: 346 x 461 micron

Figure 5

Micrograph From a G.5 Emulsion Showing Another Triplet of Heavy Tracks

Field Size 117 x 186 microns

Figure 6

Micrograph From a G.5 Emulsion Showing Heavy Track with Estimated Z = 20

Field Size: 114 x 223 microns

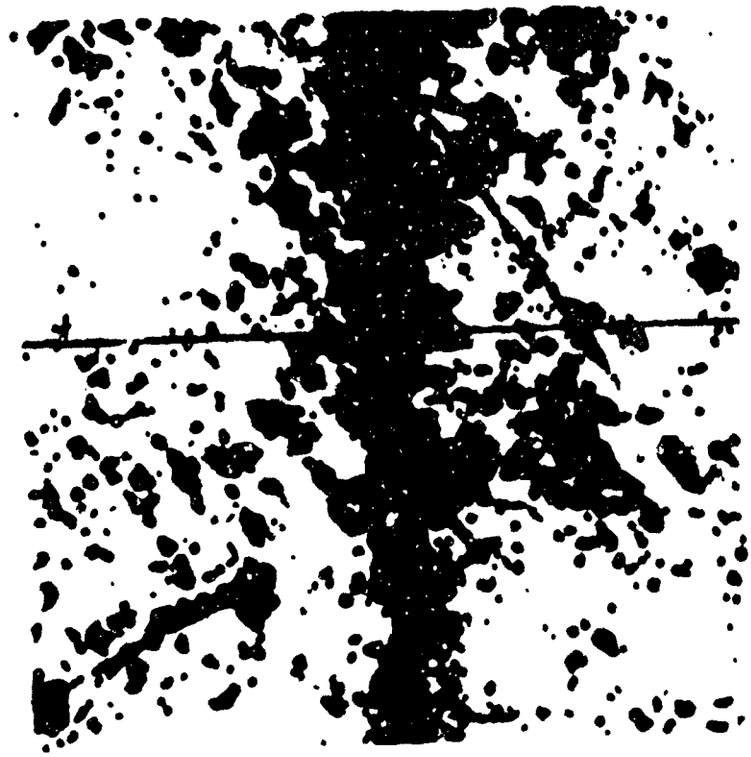

Figure 7

Micrograph From a G.5 Emulsion Showing the Heaviest Track Recorded on the Mission. Estimated Z = 28 to 30.

Field Size: 92 x 95 micron

Figure 8

Micrograph From a G.5 Emulsion Showing Heavy Track Traversing Emulsion at a Steep Angle. Estimated Z = 22 to 26.

Note disintegration star in upper part of the field.

Field Size: 203 x 230 micron

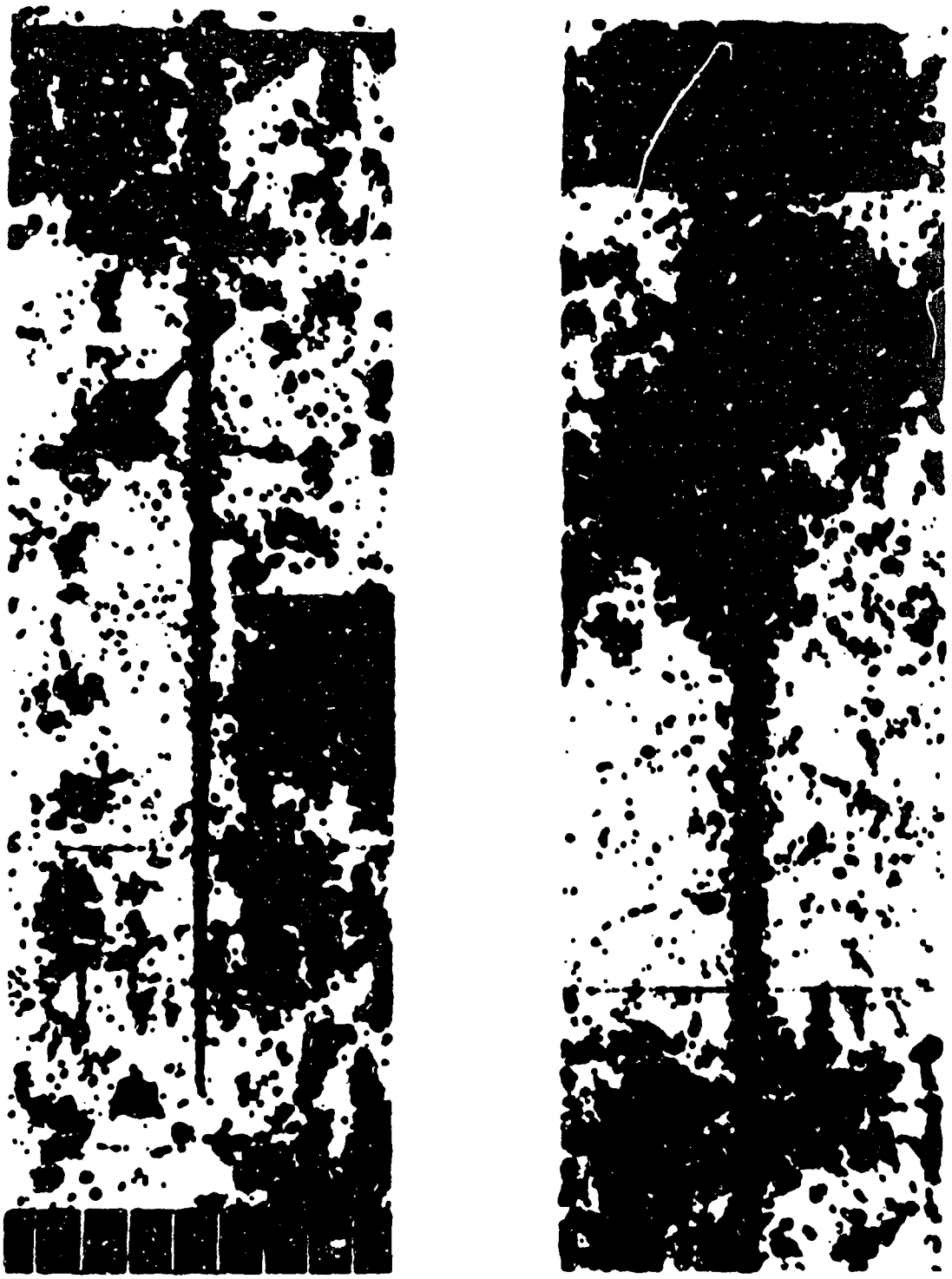

1 Division = 10 micron

Figure 9

Terminal Section ("Thindown") of a Heavy Track in a K.2 Emulsion. Estimated Z ≈ 22. Lower right connects to upper left corner.

Figure 10

"Upstream" Continuation of Track Shown in Figure 9

Four sections in Figures 9 and 10 show coherent track with lower ends connecting to adjacent upper left corner.

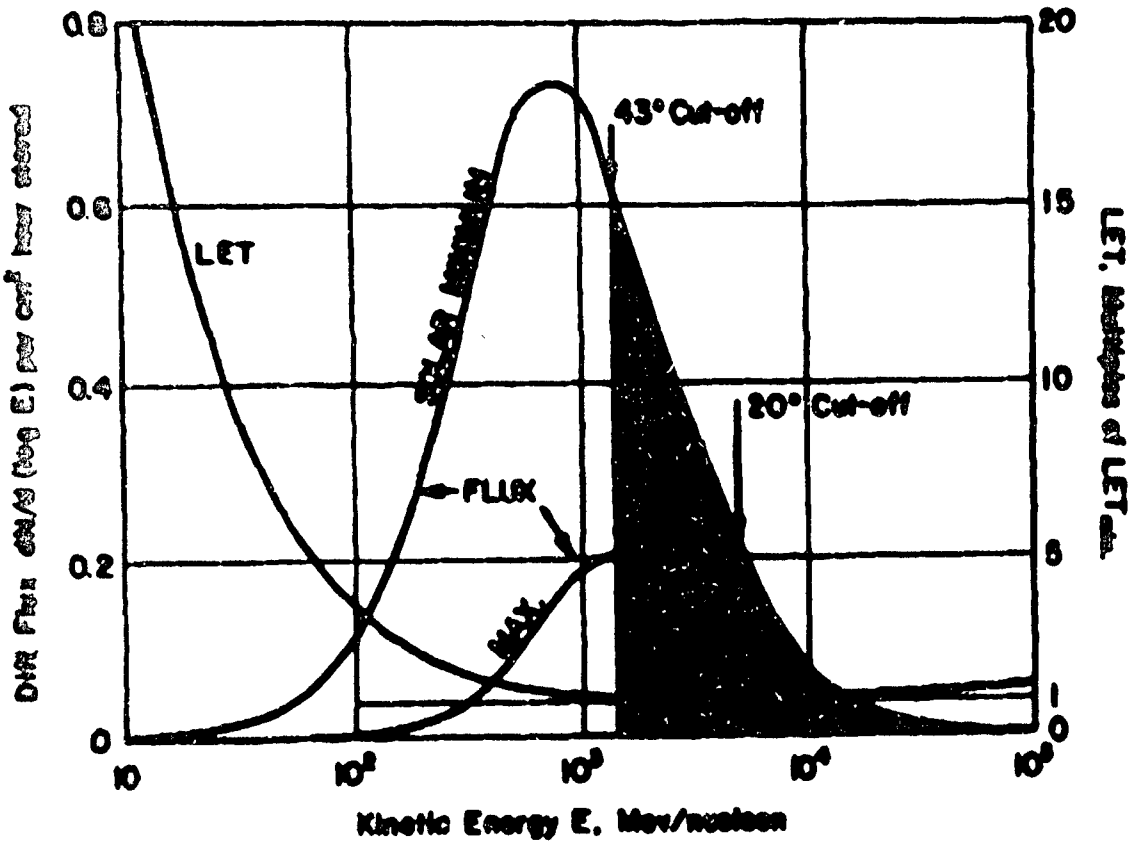

Figure 11

Differential Energy Spectra of Galactic Primaries of Z ≥ 20 at Solar Minimum and Maximum

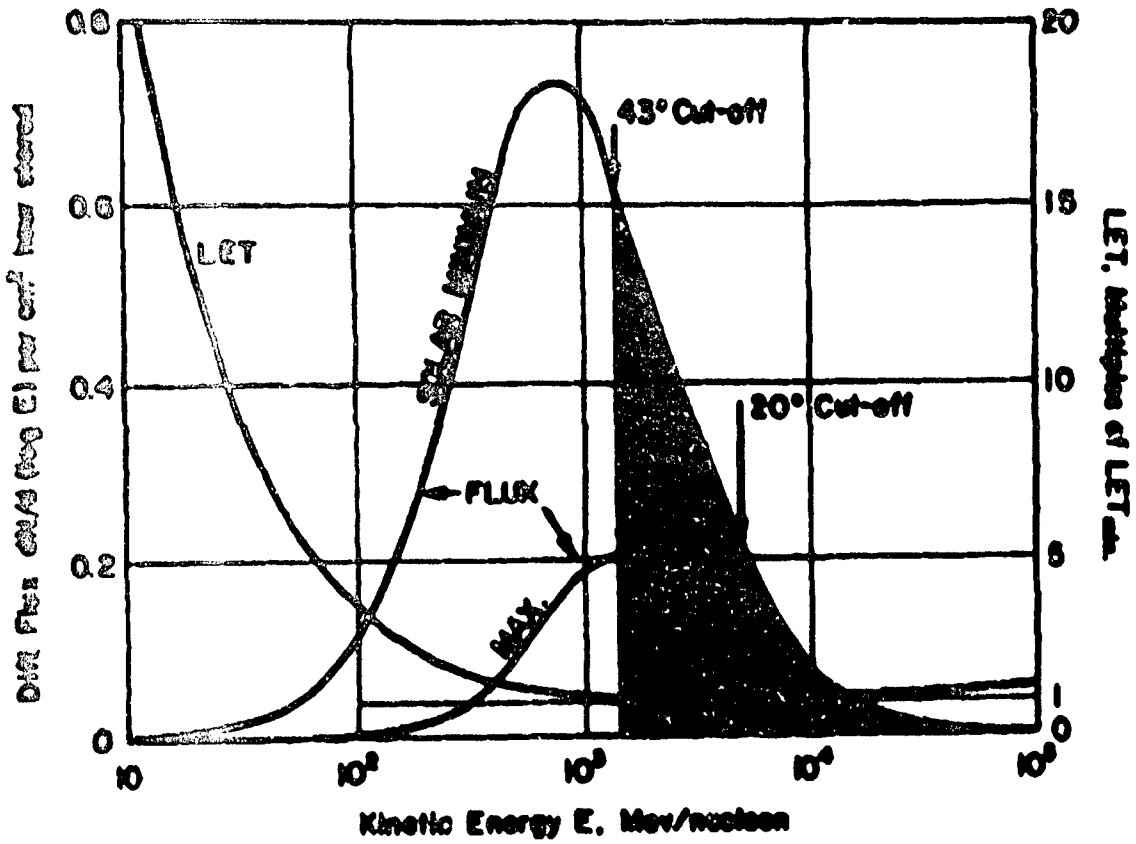

Figure 11

Differential Energy Spectra of Galactic Primaries of Z ≥ 20 at Solar Minimum and Maximum

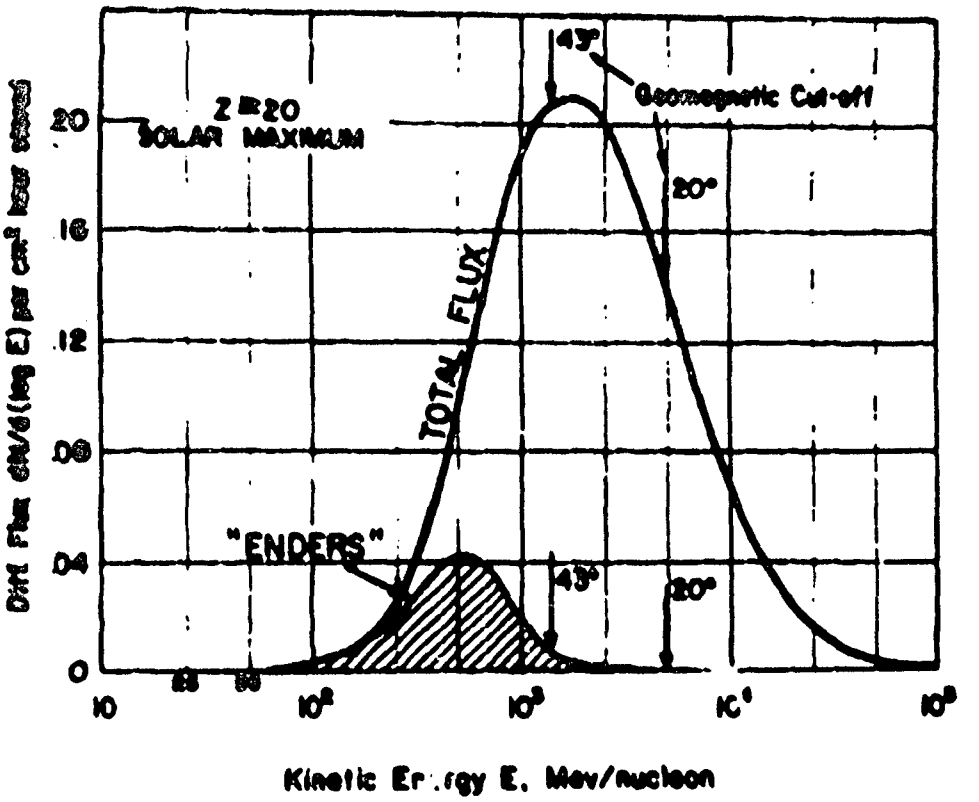

Figure 12

Differential Energy Spectra of Total and Enders Flux of Galactic Primaries of Z ≥ 20 at Solar Maximum

Unclassified

Security Classification

DOCUMENT CONTROL DATA - R & D

(Security classification of title, body of abstract and indexing annotation must be entered when the overall report is classified)

1. ORIGINATING ACTIVITY (Corporate author) Naval Aerospace Medical Research Laboratory Pensacola, Florida 32512	2a. REPORT SECURITY CLASSIFICATION Unclassified
	2b. GROUP N/A

3. REPORT TITLE

NUCLEAR EMULSION RECORDINGS OF THE ASTRONAUTS' RADIATION EXPOSURE ON THE FIRST LUNAR LANDING MISSION APOLLO XI

4. DESCRIPTIVE NOTES (Type of report and inclusive dates)

N/A

5. AUTHOR(S) (Last name, first name, initial, last name)

Hermann J. Schaefer and Jeremiah J. Sullivan

6. REPORT DATE 29 June 1970	7a. TOTAL NO. OF PAGES 28	7b. NO. OF REFS 16
8a. CONTRACT OR GRANT NO.	9a. ORIGINATOR'S REPORT NUMBER(S) NAMRL-1112	
b. PROJECT NO. MF12.524.010-5010	9b. OTHER REPORT NO(S) (Any other numbers that may be assigned this report) 46	

10. DISTRIBUTION STATEMENT

This document has been approved for public release and sale; its distribution is unlimited.

11. SUPPLEMENTARY NOTES John Report with MSC, Houston, Texas	12. SPONSORING MILITARY ACTIVITY

13. ABSTRACT

Nikl G.5 and K.2 emulsions in radiation packs carried by the astronauts on Apollo XI in their space suits were analyzed for identifying the various components of the radiation field in space and determining the total mission dose. In terms of dose equivalents, trapped protons in the radiation belt, disintegration stars in tissue, galactic heavy primaries, electrons, and neutrons contribute in that order to a total mission dose of 201 millirad or 402 millirem. In this exposure, the high-Z particles with LET values up to 3400 kev/micron tissue constitute a radiobiologically unknown quantity since it is generally agreed upon that microbeam effects in tissue cannot be measured adequately with conventional dosimetric units. Assuming that the effects in question are limited to nuclei of Z = 22 and higher, one arrives at a total mission flux of 76 nuclei/cm^2 measured on the body of the astronauts; this cannot be properly assessed in its biological significance.

DD FORM 1473 (PAGE 1)

S/N 0101-807-6801

Unclassified

Security Classification

Best Available Copy

Unclassified
Security Classification

14. KEY WORDS	LINK A ROLE	LINK A WT	LINK B ROLE	LINK B WT	LINK C ROLE	LINK C WT
Radiation hazards in space						
Space radiation dosimetry with nuclear emulsion						
Radiation exposure on Apollo XI						

DD FORM 1 NOV 65 1473 (BACK)
(PAGE 2)

Unclassified
Security Classification